Solvothermal Synthesis of Co-doped ZnO Nanopowders

Janusz Fidelus[a], Radu Robert Piticescu[b], Roxana Mioara Piticescu[b], Witold Lojkowski[a], and Liviu Giurgiu[c]

[a] High Pressure Physics Centre of the Polish Academy of Science, Sokolowska 29/37, Warsaw, Poland

[b] National Research & Development Institute for Non-ferrous and Rare Metals, 102 Biruintei Blvd, Pantelimon, Ilfov, Romania

[c] National Institute for the Research & Development of Isotopic and Molecular Technology, 65-103 Donath Str. Cluj-Napoca, Romania

Reprint requests to R. R. Piticescu. E-mail: rpiticescu@imnr.ro

Results are presented on the microwave solvothermal synthesis of Co-doped ZnO powders starting from zinc and cobalt acetate precursors in ethylene glycol solutions. The method yields powders with a relatively high degree of agglomeration of initially nucleated nanometer grains. It has been demonstrated that the thermodynamic estimations of the final composition using the Gibbs calculation method are in good agreement with experimental values for the chemical composition in a range of cobalt concentrations up to 15 mol-%.

Key words: Solvothermal Synthesis, Thermodynamic Equilibrium, Co-ZnO Nanopowders

Introduction

Several papers reported on microwave (MW) driven hydrothermal synthesis of nano-sized powders [1 – 5] at elevated pressures. The interest in these synthetic methods is stimulated by some reports on the acceleration of chemical reaction rates that can be explained in terms of local superheating of the fluids during microwave heating [6 – 8]. The application of reactors for the hydrothermal [9, 10] and solvothermal [11 – 14] synthesis, in which it is possible to utilize microwaves under increased pressure up to 12 MPa, permits to control the grain size and degree of crystallinity (*i. e.* a minimization of the content of amorphous phases, hydroxides, or unreacted remains of *e. g.* organic salts). Due to the conditions of high purity, hydrothermal microwave reactions are especially advantageous for the synthesis of doped nanopowders, which are usually obtained in a microwave reactor.

ZnO has found many applications in different areas such as building materials (paints), the production of tires, cosmetics (UV filter in creams) and food (component of feeds for animals). It is a semiconductor of high chemical and thermal stability, with an energy gap of about 3.5 eV. Due to this, ZnO efficiently absorbs ultraviolet light, and as a result of recombination of holes and electrons emits ultraviolet light in the blue region [15, 16]. Intense studies were carried out on the magnetic, spintronic and optical properties of ZnO doped with magnetic ions, doped ZnO being one of the materials in which ferromagnetism at r. t. can be observed [17 – 20]. The results of numerous investigations on the synthesis and properties of ZnO-based magnetic powders doped with transition-metal ions have been published [21 – 28].

To the best of our knowledge the use of solvothermal decomposition of metal acetates in ethylene glycol in a microwave reactor to yield nanometric doped solid metal oxides is not known.

The purpose of the present studies was to show that in the microwave reactor under solvothermal conditions it is possible to obtain ZnO nanopowders doped with Co^{2+} for studying their spin electronic resonance properties.

Thermodynamic Prediction of Solvothermal Reactions for the Synthesis of Doped ZnO

It is known that ZnO crystallizes in an AB structure of zincite and may be doped with metal ions of the 4d
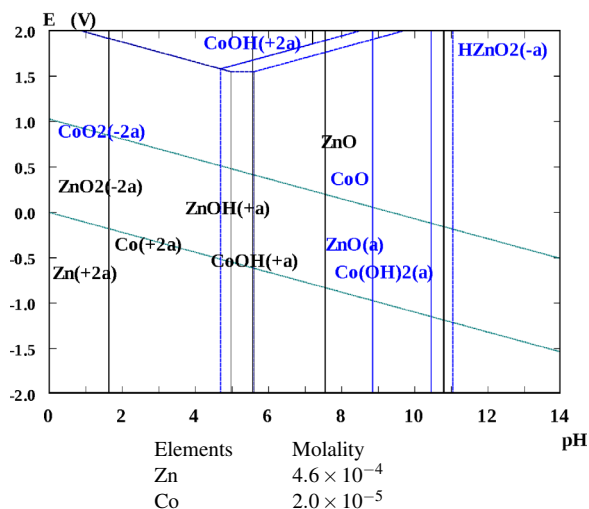
Elements	Molality
Zn	4.6×10^{-4}
Co	2.0×10^{-5}

Fig. 1. *E*-pH diagram of the system Zn-Co-H$_2$O in solvothermal solutions at 280 °C showing predominance domains of species.

elements of the Periodic Table. The possibility of introducing a dopant into the ZnO structure is dependent on the radius of the ion to be introduced into the structure. Assuming that the difference between the radius of the Co^{2+} ions (0.0745 nm) and Zn^{2+} ions (0.074 nm) is only 0.68 % (much lower than the limit of 15 % proposed by the Hume-Rothery law), it may be assumed that incorporation of Co^{2+} ions in concentration levels not exceeding 5 mol-% may replace Zn^{2+} in the ZnO crystal structure without a significant change in the lattice parameters.

A thermodynamic simulation was performed using the soft HSC Chemistry version 6-Outokumpu, Finland, considering the possible reaction (a = aqueous):

$$ZN(CH_3COO_2)(a) + CO(CH_3COO)_2(a) \xrightarrow{C_2H_4(OH)_2(a)}$$

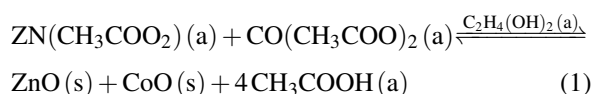$$ZnO(s) + CoO(s) + 4CH_3COOH(a) \qquad (1)$$

Fig. 1 shows the thermodynamic prediction of the phase equilibria during the solvothermal processes using the Pourbaix diagram considering the experimental concentration of Zn(II) and Co(II) in the solution and the real ionic strength.

This diagram was calculated for the system ZnO-5 mol-% CoO in solvothermal solutions at 280 °C. The pH required for complete precipitation of both oxides (CoO*ZnO) is in the range from 7.6 to 11.6 at 280 °C. Fig. 2 shows the calculated equilibrium compositions for the system. One can see that it is possible to obtain ZnO-5 mol-% Co at a temperature higher
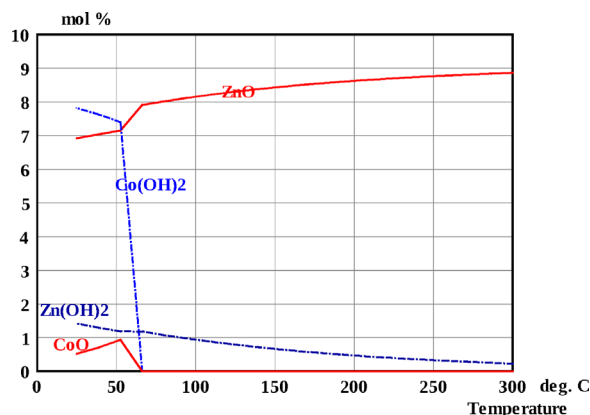

Fig. 2. Equilibrium composition diagram (Gibbs calculations) for the system ZnO-5 mol-% Co.

than 260 °C. Above this temperature the hydroxides disappear.

Experimental Section

The metal acetates were purchased from Aldrich and used without further purification.

A mixture of cobalt and zinc acetates was weighted in a ratio corresponding to the desired stoichiometry of CoO in ZnO and dissolved in 50 mL of either water or ethylene glycol. The aqueous solutions were heated to 150 °C, while the ethylene glycol reactions were carried out at 280 °C in a microwave MARS 3 reactor. The duration of the reaction was 40 min and the pressure was kept at 2 MPa. The microwave power in all reactions was 300 W. At the end of the reaction the product was filtered, washed five times with ethanol, centrifuged and dried in vacuum for 24 h. The composition of the Co-doped ZnO solids was determined using ICP spectrometry.

The X-ray diffraction (XRD) patterns were collected in the 2θ range of $20-90°$ at r. t., with a step of 0.05° using a Bruker D8 Advance diffractometer operating with CuK_α radiation, while the real chemical composition of the Co-doped ZnO powders was measured by an Inductively Coupled Plasma Spectrometer (ICP-Spectroflame, Germany). The density measurements were carried out by means of a helium pycnometer (AccuPyc 1330 Micrometrics), and the specific surface area (BET measurements) by means of Gemini Micrometrics. Each material was subjected to desorption at 150 °C for 2 h prior to the measurement.

The grain shape, size and degree of agglomeration of the synthesized powders were analyzed by means of a scanning electron microscope SEM LEO 1530. Studies were carried out for materials obtained from the solution concentration of 10 mol-% of the dopant ion. Electron spin resonance (ESR) spectra of Co-doped ZnO nanopowders were recorded using
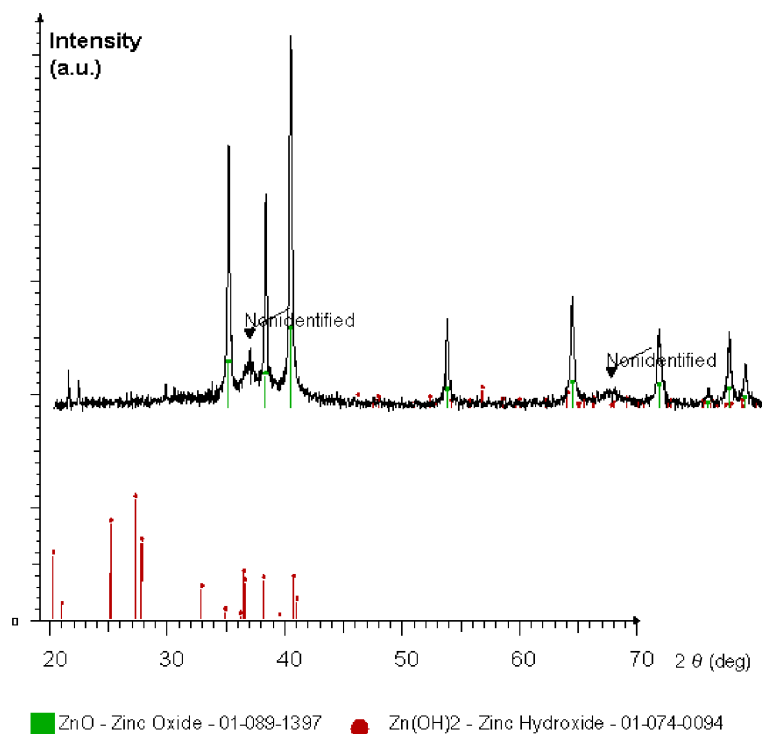
Table 1. Results of chemical analyses and of specific surface area and density measurements of Co-doped ZnO powders.

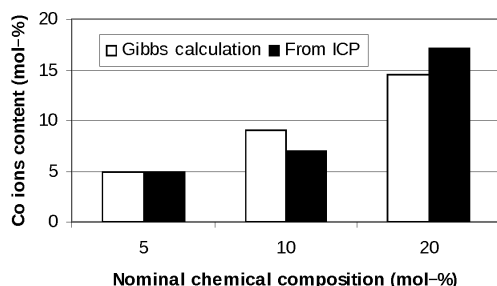| Sample code	CoO content (mol-%)	BET ($m^2\,g^{-1}$)	Density ($g\,cm^{-3}$)
ZnO	0	34.20	5.09
0.001 CoZnO	0.001	32.90	5.10
0.01 CoZnO	0.012	31.50	5.15
5 CoZnO	5.05	22.70	5.25
10 CoZnO	10.10	21.00	5.28
15 CoZnO	15.36	21.00	5.35

Fig. 4. Comparison between Co (in mol-%) experimentally measured and computed from Gibbs calculations in Co-doped ZnO powders synthesized under microwave-driven solvothermal conditions.

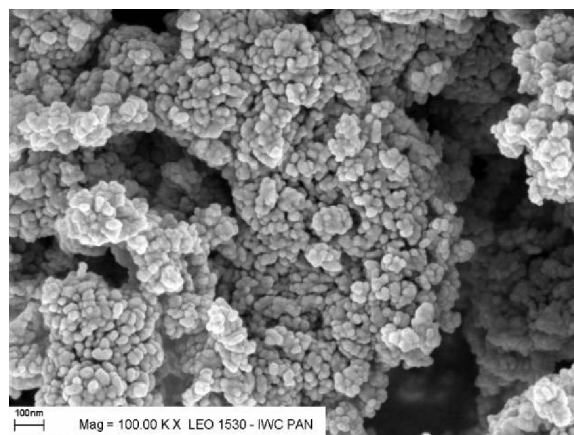a SEX-Radiopan apparatus operating in the X frequency band.

Fig. 5. SEM micrograph of ZnO nanopowders doped with 10 mol-% Co.

Results and Discussions

The chemical compositions in mol-% calculated from ICP measurements, the BET specific area and the density of Co-doped ZnO powders synthesized in a microwave reactor in ethylene glycol are presented in Table 1. The purity of the products was confirmed by density studies by means of a helium pycnometer. The

Table 2. ESR spectral parameters (*g* factor and band width) calculated from electron spin resonance spectra.

$Zn_{1-x}Co_xO$	$g_\parallel$	$g_\perp$	ΔH
$x = 0.001$	2.765	11.579	1033
$x = 0.01$	2.765	10.769	1085

specific surface BET of the powders obtained is lower compared to that obtained under identical conditions with pure, undoped ZnO.

The XRD analysis of ZnO powders doped with Co is presented in Fig. 3, showing the formation of ZnO as a major phase (97 %), the rest of about 3 % being $Zn(OH)_2$ even at higher Co concentration. A small amount (less than 1 %) of an unidentified compound is also observed.

Fig. 4 presents a comparison between the chemical composition of the dopant (in mol-%) experimentally measured by ICP and thermodynamically predicted from Gibbs calculations. It is clear that Co^{2+} ions are easily incorporated into the ZnO structure as shown by both theoretical and experimental studies. The amount of Co at the level of 5 mol-% obtained from ICP and Gibbs calculations is near the nominal chemical composition.

The morphology of a Co-doped ZnO nanopowder containing theoretically 10 mol-% dopant is presented in Fig. 5. A relatively high degree of agglomeration of initially nucleated nanometer grains is observed.

The ESR parameters for ZnO powders at low levels of Co dopant are presented in Table 2.

The values are typical for Co^{2+} ions with axial symmetry. In the temperature range 4 – 200 K the *g* factor and the band width are independent of temperature. With increasing Co^{2+} dopant concentration, the band width increases due to increasing bipolar interactions in the system.

Conclusions

The microwave-driven solvothermal process provides fast heating of the reactants and an accelerated reaction rate and allows the preparation of nanocrystalline doped powder with a high dopant concentration. In the case of doping with Co^{2+} ions, doping up to the 15 mol-% level (from ICP) was achieved. The powders have a crystalline structure corresponding to zinc oxide, with about 3 % zinc hydroxide originating from unreacted starting materials as well as new phases that should be further investigated.

In the absence of reliable phase diagrams for the studied systems it is concluded that thermodynamic simulations are very useful for studies of solvothermal methods driven by microwaves. The experiments confirm the high potential offered by solvothermal chemistry in producing oxides with increased dopant concentrations due to the *in situ* concomitant nucleation of oxides, as observed from ESR spectra. However, future work is required to establish if surface segregation processes occur in the proposed systems.

[1] F. Bondioli, A. M. Ferrari, S. Braccini, C. Leonelli, G. Pellacani, A. Opalinska, T. Chudoba, E. Grzanka, B. Palosz, W. Lojkowski, *Solid State Phen.* **2003**, *94*, 193 – 196.

[2] S. Somiya, T. Akiba, *J. Eur. Ceram. Soc.* **1999**, *19*, 81 – 87.

[3] F. Bondioli, C. Leonelli, C. Siligardi, G. Pellacani, S. Komarneni, *Report 8th Int. Symposium on Microwave and High Frequency Processing*, Springer Verlag, Berlin **2002**.

[4] S. Komarneni, R. Pidugu, Q. H. Li, R. Roy, *J. Mater. Res.* **1995**, *10*, 1687 – 1692.

[5] J. R. Huang, Z. X. Xiong, C. Fang, B. L. Feng, *Mater. Sc. & Eng. B* **2003**, *99*, 226 – 229.

[6] D. M. P. Mingos, D. R. Baghurst, *Chem. Soc. Rev.* **1991**, *20*, 1 – 47.

[7] D. M. P. Mingos, *Res. Chem. Intermed.* **1994**, *20*, 85 – 91.

[8] A. G. Whittaker, D. M. P. Mingos, *J. Microwave Power Electromagn. Energy* **1994**, *29*, 195 – 219.

[9] K. Kamata, H. Hosono, Y. Maeda, K. Miyokawa, *Chem. Lett.* **1984**, 2021 – 2022.

[10] T. Strachowski, E. Grzanka, B. Palosz, A. Presz, L. Slusarski, W. Lojkowski, *Solid State Phen.* **2003**, *94*, 189 – 192.

[11] O. Palchik, I. Felner, G. Kataby, A. Gedanken, *J. Mater. Res.* **2000**, *15*, 10.

[12] O. Palchik, R. Kerner, Z. Zhu, A. Gedanken, *J. Solid State Chem.* **2000**, *154*, 520 – 534.

[13] O. Palchik, J. Zhu, A. Gedanken, *J. Mater. Chem.* **2000**, *10*, 1251 – 1254.

[14] J. Zhu, O. Palchik, S. Chen, A. Gedanken, *J. Phys. Chem. B* **2000**, *104*, 7344 – 7347.

[15] Y. Chen, D. Bagnall, T. Yao, *Mater. Sci. Eng.* **2000**, *B 75*, 190.

[16] D. C. Look, *Mater. Sci. Eng.* **2001**, *B 80*, 383.

[17] T. Dietl, H. Ohno, F. Matsukura, J. Cibert, D. Ferrand, *Science* **2000**, *287*, 1019.

[18] A. Guptab, F. J. Owensc, A. Inoued, K. V. Raob, *J. Magn. Magn. Mater.* **2004**, *282*, 115 – 121.

[19] C.-H. Chien, S. H. Chioub, G. Y. Guoa, Y.-D. Yaoc, *J. Magn. Magn. Mater.* **2004**, *282*, 275 – 278.

[20] H. J. Blythe, R. M. Ibrahim, G. A. Gehring, J. R. Neal, A. M. Fox, *J. Magn. Magn. Mater.* **2004**, *282*, 117 – 127.

[21] D. H. Zhang, Z. Y. Xue, Q. P. Wang, *J. Phys. D: Appl. Phys.* **2002**, *35*, 2837.

[22] H. Hayashi, A. Ishizaka, M. Haemori, H. Koinuma, *Appl. Phys. Lett.* **2003**, *82*, 1365.

[23] Z. Zhou, K. Katoa, T. Komakia, M. Yoshinoa, H. Yukawaa, M. Morinagaaand, K. Moritab, *J. Europ. Ceram. Soc.* **2004**, *24*, 139 – 146.

[24] H. J. Blythe, R. M. Ibrahim, G. A. Gehring, J. R. Neal, A. M. Fox, *J. Magn. Magn. Mater.* **2004**, *283*, 117 – 127.

[25] S. Liu, K. Takahashi, K. Uematsu, M. Ayabe, *Appl. Catal. A* **2004**, *277*, 265 – 270.

[26] S. V. Bhat, F. L. Deepak, *Solid State Commun.* **2005**, *135*, 345 – 347.

[27] M. Ghosh, R. Seshadri, *J. Nanosci. Nanotechn.* **2004**, *4*, 136 – 140.

[28] D. P. Joseph, G. S. Kumar, C. Venkateswaran, *Mater. Lett.* **2005**, *59*, 2720 – 2724.